




## RESEARCH REPORT

WILEY

# Morphofunctional characterisation of axonal damage in different rat models of chemotherapy-induced peripheral neurotoxicity: The role of nerve excitability testing

Alessia Chiorazzi<sup>1,2</sup> | Annalisa Canta<sup>1,2</sup> | Valentina Alda Carozzi<sup>1,2</sup> |  
Cristina Meregalli<sup>1,2</sup>  | Eleonora Pozzi<sup>1,2</sup> | Elisa Ballarini<sup>1,2</sup> |  
Virginia Rodriguez-Menendez<sup>1,2</sup> | Paola Marmioli<sup>1,2</sup> | Guido Cavaletti<sup>1,2,3</sup>  |  
Paola Alberti<sup>1,2,3</sup> 

<sup>1</sup>Experimental Neurology Unit, School of Medicine and Surgery, Monza, Italy

<sup>2</sup>NeuroMI (Milan Center for Neuroscience), Milan, Italy

<sup>3</sup>Fondazione IRCCS San Gerardo dei Tintori, Monza, Italy

## Correspondence

Paola Alberti, School of Medicine and Surgery, University of Milano-Bicocca, Asclepio Building, 1st floor, Room 1034, Via Cadore, 48, 20900 Monza (MB), Italy.  
Email: [paola.alberti@unimib.it](mailto:paola.alberti@unimib.it)

## Abstract

**Background and Aims:** Chemotherapy-induced peripheral neurotoxicity (CIPN) is a common and long-lasting adverse event of several anticancer compounds, for which treatment has not yet been developed. To fill this gap, preclinical studies are warranted, exploiting highly translational outcome measure(s) to transfer data from bench to bedside. Nerve excitability testing (NET) enables to test *in vivo* axonal properties and can be used to monitor early changes leading to axonal damage.

**Methods:** We tested NET use in two different CIPN rat models: oxaliplatin (OHP) and paclitaxel (PTX). Animals (female) were chronically treated with either PTX or OHP and compared to respective control animals. NET was performed as soon as the first injection was administered. At the end of the treatment, CIPN onset was verified via a multimodal and robust approach: nerve conduction studies, nerve morphometry, behavioural tests and intraepidermal nerve fibre density.

**Results:** NET showed the typical pattern of axonal hyperexcitability in the 72 h following the first OHP administration, whereas it showed precocious signs of axonal damage in PTX animals. At the end of the month of treatment, OHP animals showed a pattern compatible with a mild axonal sensory polyneuropathy. Instead, PTX cohort was characterised by a rather severe sensory axonal polyneuropathy with minor signs of motor involvement.

**Interpretation:** NET after the first administration demonstrated the ongoing OHP-related channelopathy, whereas in PTX cohort it showed precocious signs of axonal damage. Therefore, NET could be suggested as an early surrogate marker in clinical trials, to detect precocious changes leading to axonal damage.

This is an open access article under the terms of the [Creative Commons Attribution-NonCommercial-NoDerivs](https://creativecommons.org/licenses/by-nc-nd/4.0/) License, which permits use and distribution in any medium, provided the original work is properly cited, the use is non-commercial and no modifications or adaptations are made.

© 2023 The Authors. *Journal of the Peripheral Nervous System* published by Wiley Periodicals LLC on behalf of Peripheral Nerve Society.

**KEYWORDS**

axonal damage, chemotherapy-induced peripheral neuropathy, chemotherapy-induced peripheral neurotoxicity, histopathology, nerve excitability testing

## 1 | INTRODUCTION

Chemotherapy-induced peripheral neurotoxicity (CIPN) is a common and potentially long-term/persistent adverse event of the most commonly used anticancer drugs: platinum drugs, taxanes, vinca alkaloids, proteasome inhibitors and thalidomide.<sup>7</sup> There is no state of the art efficacious curative and/or preventive treatment for this condition.<sup>19,22,31,38</sup>

In part, this unmet clinical and scientific need is due to an incomplete understanding of axonal damage mechanisms related to different anticancer drugs.<sup>28</sup> Therefore, it is crucial to have robust preclinical models addressing pathogenetic mechanisms.<sup>15</sup> In this regard *in vivo* models are pivotal and it is mandatory to use translational methods to promptly transfer data from bench to bedside and vice versa; nerve conduction studies (NCS) are quite a relevant option since they can be similarly performed at a preclinical and clinical level in CIPN.<sup>1,3,6,9,17,26,27,34</sup> However, an even more refined option can lead to deeper investigations on axonal damage mechanisms: nerve excitability testing (NET). NET is an elegant approach that enables testing axonal properties; it was first devised in a clinical setting<sup>13,16</sup> and later adapted to animal models.<sup>11,14,24,40</sup> In investigating CIPN, it raised increasing interest and application in oxaliplatin(OHP)-induced CIPN since NET can detect the hyperexcitability state that OHP can transiently induce, on the side of the chronic cumulative axonal polyneuropathy,<sup>2</sup> both at a clinical<sup>18,20,21,30</sup> and preclinical<sup>5,12,23</sup> level. However, NET could be also used to verify other early changes leading to axonal damage due to different anticancer drugs, possibly detecting precocious alterations. In CIPN NET was little explored apart from the OHP-related setting; only a small study on a clinical cohort was published suggesting that NET can detect early changes due to antitubulinic agent.<sup>29</sup> To further explore NET exploitability to test CIPN pathogenesis, we therefore used NET in two different robust CIPN models, one related to platinum compounds, OHP, and the other to an antitubulinic agent, paclitaxel (PTX), whose neurotoxic patterns are quite different: platinum compounds first target dorsal root ganglia (DRG) neurons and cause a mild sensory axonal neuronopathy, whereas, PTX, thanks to its effects on microtubules, exerts a relevant damage in axons leading to a moderate-severe sensory-motor axonal polyneuropathy.<sup>7,28</sup> Our aim was to explore NET use in CIPN setting to exploit its full potential in monitoring early alterations related to different mechanisms underlying axonal damage.

## 2 | MATERIALS AND METHODS

Experiments were conducted in accordance with ARRIVE 2.0 guidelines.<sup>32</sup>

### 2.1 | Animal and housing

Forty female Wistar rats (Envigo, Bresso, Italy) weighing 175–200 grams at the beginning of the study were used. The care and husbandry of animals were in conformity with the institutional guidelines in compliance with national (D.L. n. 26/2014) and international laws and policies (Directive 2010/63/EU of the European Parliament and of the Council, 2010; Guide for the Care and Use of Laboratory Animals, US National Research Council, 8th ed., 2011). Animals were housed in an animal facility where room temperature and relative humidity were set at  $20 \pm 2^\circ\text{C}$  and  $55 \pm 10\%$ , respectively and artificial lighting provided a 12 h light/12 h dark (7 a.m.–7 p.m.) cycle. Rats were housed in an adequate cage with rodent diet and water *ad libitum*, subjected to daily monitoring of their clinical conditions. Body weight was monitored twice a week to ensure animal well-being and to ensure drug dose adjustments, on the basis of the weight. Animal well-being was daily assessed via clinical monitoring. All procedures were approved by the Italian Ministry of Health (authorisation n°1161/2016-PR, 12/12/ 2016).

### 2.2 | Study design and sample size

Sample size for each experiment was calculated on the basis of nerve conduction velocity (NCV) reference values of our laboratory,<sup>5,26,27</sup> assuming that the relevant difference between control and OHP groups is 5 m/s (standard deviation = 7); thus, if a 2-sided 5% alpha and a 80% power is set, the sample size is seven animals/group ([www.dssresearch.com/KnowledgeCenter/toolkitcalculators/samplesizecalculators.aspx](http://www.dssresearch.com/KnowledgeCenter/toolkitcalculators/samplesizecalculators.aspx)). In each experiment, the sample size was slightly increased above this number in order to have enough animals to be tested at each time point, in case of animal loss due to chemotherapy administration. Animals were randomised at baseline via results of NCS values. After the first administration, NET was performed in all animals. Upon treatment completion, all animals underwent behavioural testing and then NCS. After sacrifice samples from at least three animals/group were obtained for histopathological analyses.

### 2.3 | Treatment groups and drugs

As stated above, animals were divided into two different studies. In the OHP study rats were divided into two groups of eight animals each. In the first group the animals were untreated while the animals in the second group were treated with OHP 5 mg/kg twice a week for 4 weeks. Oxaliplatin (TEVA, Pharma B.V., Mijdrecht, The Netherlands) was administered by intravenous injection. In the PTX

study 24 rats were used and divided into two groups of 12 animals each; the numerosity per group was slightly higher in this study since PTX injection can more easily damage rat tails, thus, preventing neurophysiological recordings as further described. Control animals were untreated while group 2 consisted of animals treated with PTX 10 mg/kg once a week for 4 weeks. Paclitaxel (LC Laboratories, Woburn, MA) was administered by intravenous injection and dissolved in a vehicle solution composed by 10% tween 80, 10% EtOH absolute and 80% saline solution.

## 2.4 | Behavioural tests

In order to evaluate thermal (cold) and mechanical sensitivity Cold Plate test and Dynamic test were performed respectively; at the end of treatment Cold Plate test was performed in both studies, whereas in PTX experiments also Dynamic test for mechanical allodynia was performed given the different clinical profile of PTX-related CIPN, in which cold-induced painful manifestations are less represented.<sup>7</sup> The cold sensitivity was assessed using the Cold Plate apparatus (model 35 100—Hot/Cold Plate, Ugo Basile Biological Instruments, Comerio, Italy) composed by a lexiglass cylinder and a thermostatic plate. In our study the plate was set at +4°C. During the test, each rat was placed in the Plexiglass cylinder free to move and walk and the number of pain signs/suffering (jumping, hind paws lifts and licking) was recorded in a trial of 5 min. The trial was suspended before the end if the animal presented signs of a strong sensitivity showing anxiety and vocalising. The mechanical threshold was assessed using Dynamic Aesthesiometer apparatus (model 37 450—Dynamic Plantar Aesthesiometer, Ugo Basile Biological Instruments, Comerio, Italy). A pointed metallic filament with 0.5 mm diameter was applied to the plantar surface of the hind paw and exerted a progressively increasing pressure reaching up to 50 g within 20 s. Paw withdrawal latencies were recorded alternatively on each side every 2 min on three occasions to yield a mean value and the results represented the maximal pressure tolerated by the animals. In order to avoid skin damage the cut-off was set at 20 s.

## 2.5 | Morphology—caudal nerves

The distal caudal nerve specimens were fixed for 3 h at room temperature in glutaraldehyde 3%, post-fixed in OsO<sub>4</sub> and epoxy resin embedded. Morphological and morphometric analyses were carried out on 1.5 µm-thick semi-thin sections stained with methylene blue. At least three tissue blocks for each animal were sectioned and then examined with a Nikon Eclipse E200 light microscope (Leica Microsystems GmbH, Wetzlar, Germany).

## 2.6 | Intraepidermal nerve fibre density (IENFD)

At the end of the treatment skin biopsies were collected and fixed in PLP (2% paraformaldehyde, lysine and periodate sodium) for 24 h at

4°C and then cryoprotected and serially cut with a cryostat to obtain 20 µm-thick sections. Three sections for each biopsy from three animals/group were selected and immunostained with rabbit polyclonal anti-protein gene product 9.5 (PGP 9.5; GeneTex, Irvine, CA, USA) using a free-floating protocol. Under a light microscope (Nikon Eclipse E200 light microscope, Leica Microsystems GmbH, Wetzlar, Germany) the total number of PGP 9.5-positive fibres were counted in a blinded fashion. The length of the epidermis was measured and the linear density of IENF/mm was calculated.

## 2.7 | Nerve conduction studies (NCS)

Recordings were performed on all animals/groups at baseline and at the end of treatment, following our recently published protocol.<sup>27</sup> Electromyography apparatus Myto2 (ABN Neuro, Firenze, Italy) and stainless steel needle electrodes were used (Subdermal EEG needle, Ambu™, Ballerup, Denmark) for recordings. All procedures were performed under standard conditions under deep isoflurane anaesthesia; animal body temperature was monitored and kept constant at 37 ± 0.5°C with a thermal pad, electronically connected to a thermal rectal probe (Harvard Apparatus, Holliston, US). The optimal setting of stimulation for each nerve was reached following the subsequent protocol; sensory recordings were performed in an orthodromic setting. For *distal caudal nerve sensory action potential (SAP)*, the active recording electrode was placed at 5 cm from the tip of the tail and the reference recording electrode at 6 cm from it, the anode was placed at 1 cm from the tip of the tail and the cathode at 2 cm from it, the ground electrode was placed midway between the cathode and the active recording electrode. For *proximal caudal nerve SAP*, the reference recording electrode was placed at 1 cm from the base of the tail and the active recording electrode 2 cm from it, the cathode was placed at 5 cm from the base of the tail and the anode at 6 cm from it, the ground electrode was placed midway between the cathode and the active recording. For *digital nerve SAP*, the reference recording electrode was placed in front of the patellar bone, the active recording electrode close to ankle bone, the cathode was placed at the base of the fourth toe and the anode was positioned at the tip of it; the ground electrode was placed in the sole. For *caudal nerve compound muscle action potential (CMAP)*, the reference recording electrode was placed at 12 cm from the base of the tail and the active one at 11 cm from it, the ground electrode was placed at 8 cm from the base of the tail; for the distal stimulation site: the cathode was placed at 6 cm from the base of the tail and the anode at 5 cm from it, whereas for the proximal stimulation site, the cathode was placed at 2 cm from the base of the tail and the anode at 1 cm from it. Intensity, duration and frequency of stimulation were set up to obtain optimal results. For both sensory and motor recordings the peak-to-peak amplitude was considered. For sensory and motor NCV calculation, onset of SAPs and CMAPs was considered. Averaging was applied carefully. For sensory recordings filters were kept between 20 Hz and 3 KHz, for motor recordings between 20 Hz and 2 KHz. Sweep was kept at 0.5 ms.

## 2.8 | Nerve excitability testing

Methods described by Yang et al. (2000)<sup>41</sup> were followed to test *caudal nerve* CMAP. Rats were under deep isoflurane anaesthesia and body temperature was kept constant at 37  $\pm$  0.5°C. Briefly, this montage was used. For stimulation, disposable, non-polarizable, Ag-AgCl cup electrodes (Ambu®, Ballerup, Denmark) were used with the conductive EEG paste (Ten20 Conductive EEG paste, Weaver and Company, Birmingham, AL). Depilatory cream (Veet®, Slough, UK) was used for hair removal to allow positioning of the anode on the left hip. Cathode was set on the homolateral side of the tail, at 1.5 cm from its base. Skin was gently rinsed (Nuprep EEG & ECG Skin Prep Gel, Konan Medical, Irvine, CA) before placing cup electrodes, to guarantee appropriate cutaneous impedance. Stainless steel needle electrodes (Subdermal EEG needle, Ambu®, Ballerup, Denmark) were used for ground and recording electrodes: active and reference recording electrodes were set at 6 and 2 cm distally to the cathode, respectively; ground electrode was positioned midway between cathode and active recording electrode.

As stimulator, an isolated linear bipolar constant current stimulant was used (maximal output  $\pm$  10 mA, DS4, Digitimer, Welwyn Garden City, UK); the Xcell3 Microelectrode Amplifier (FHC, Bowdoin, ME) was connected to the recording electrodes via a customised probe/adaptor specifically designed by FHC for our needs; National Instrument USB-6221-BNC Acquisition Device (National Instrument Italy, Assago, Italy) was used to connect all these instruments. For NET recordings the Qtra© software (Institute of Neurology, Queen Square, London, UK) and TROND protocol were used.

## 2.9 | Statistical analysis and sample size calculation

Descriptive statistics were generated for all variables. Normally distributed data were analysed with parametric tests (*t*-test) and non-normally distributed with non-parametric tests (Mann-Whitney *U* test). Two-sided tests were used. A *p*-value < .05 was set as significant. All analyses were conducted in Graphpad environment (v4.0, La Jolla, CA, USA), apart from NET recordings. NET data were analyzed with QtraP© (Institute of Neurology, Queen Square, London, UK), the

companion of the recording software QtraS© (Institute of Neurology, Queen Square, London, UK).

## 3 | RESULTS

### 3.1 | Behavioural tests

Compared to control animals, the OHP-treated group developed cold hyperalgesia ( $p < .01$ , Figure 1A) at the end of the treatment. On the contrary, after 4 weeks of administration, PTX-treated rats did not show cold hyperalgesia (Figure 1B) but, in these animals, the onset of mechanical allodynia was observed ( $p < .0001$  vs. control group, Figure 1C).

### 3.2 | Morphology—caudal nerves

Histopathological analyses of caudal nerves were used to confirm the different severity in axonopathy that ensued in both experiments, as summarised by Figure 2. OHP-treated animals showed a mild axonopathy, as typical of this chemotherapy drug<sup>2,5,28</sup> (Figure 2B), whereas PTX-treated animals showed a rather severe axonopathy with evident axonal loss and degenerating fibres<sup>28,37,39</sup> (Figure 2D).

### 3.3 | Morphology—IENFD

At the end of the treatment, a qualitative light microscopic observation (Figure 3A, C) and a quantitative nerve fibre density assessment (Figure 3B, D) performed on skin biopsy obtained from both experiments showed a significant reduction in IENF density in both PTX- and OHP-treated animals ( $p < .0001$  vs. control group).

### 3.4 | NCS

NCS (as shown in Figure 4) mirrored information gained via morphological observations of the caudal nerves. In both experiments a

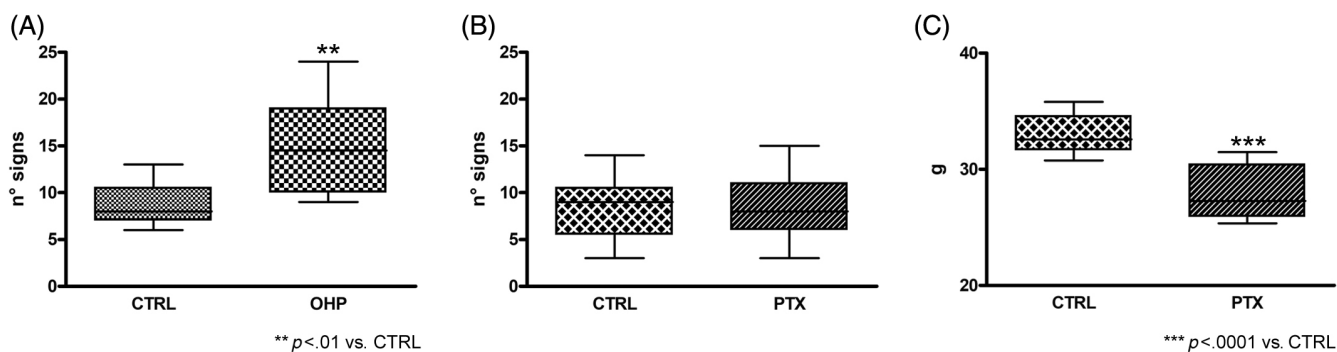


**FIGURE 1** Behavioural test results. Figure 1A: cold plate at the end of treatment in OHP experiment (y axis represents the number of painful signs recorded, after exposure to the cold stimulus). Figure 1B: cold plate test at the end of treatment in PTX experiment (y axis represents the number of painful signs recorded, after exposure to the cold stimulus). Figure 1C: dynamic test at the end of treatment in PTX experiment. \*\*: *p*-value < .01 versus control group; \*\*\*: *p*-value < .001 versus control group. CTRL, control group; OHP, oxaliplatin group; PTX, paclitaxel group.



**FIGURE 2** Caudal nerve histopathology. Figure 2A: control animal representative image in OHP experiment; Figure 2B: OHP animal representative image in OHP experiment; Figure 2C: control animal representative image in PTX experiment; Figure 2D: PTX animal representative image in PTX experiment. CTRL, control group; OHP, oxaliplatin group; PTX, paclitaxel group.

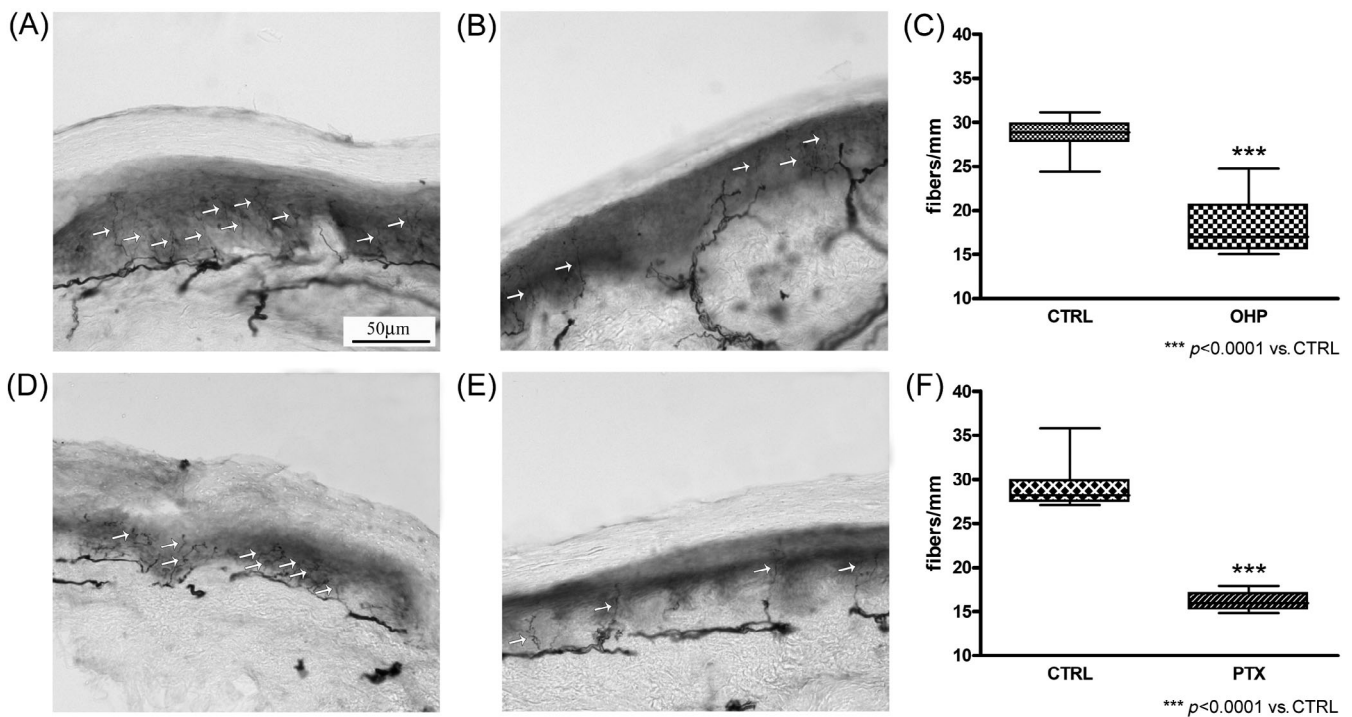
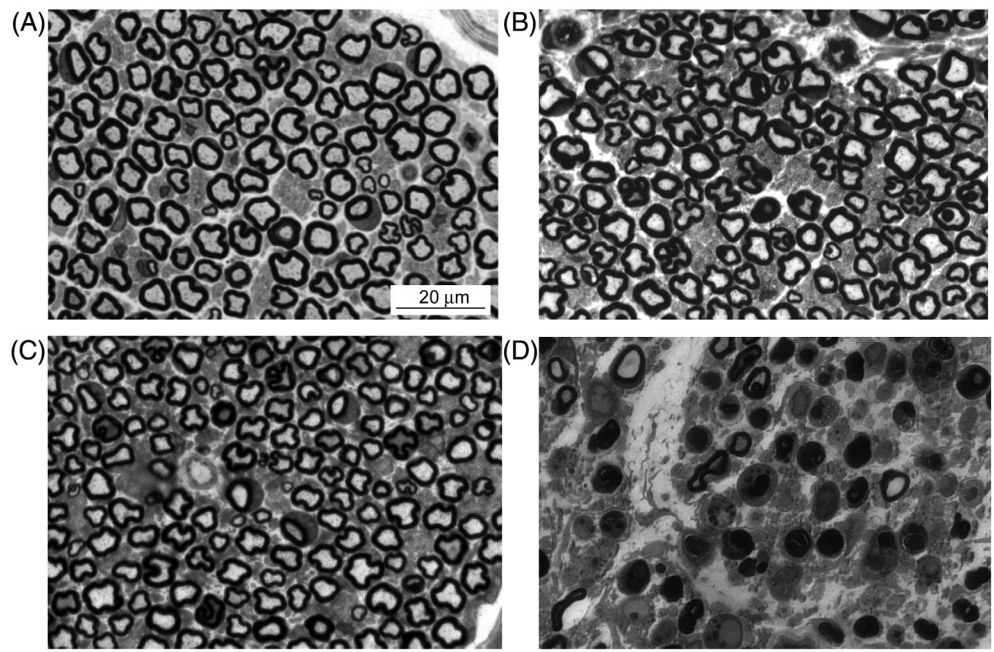


**FIGURE 3** IENFD representative images and analysis. Figure 3A, B: representative images of control (3A) and OHP (3B) group (white arrows point out intraepidermal nerve fibres); Figure 3C: statistical analysis demonstrating a significant reduction of IENFD in OHP experiment; Figure 3D, E: representative images of control (3D) and PTX (3E) animals (white arrows point out intraepidermal nerve fibres); Figure 3F: statistical analysis demonstrating a significant reduction of IENFD in PTX experiment. CTRL, control group; OHP, oxaliplatin group; PTX, paclitaxel group.

length-dependent axonopathy was demonstrated, far severer in the PTX animals than in OHP animals, with a minor motor involvement only in the PTX cohort, as expected on the basis of literature data.<sup>2,5,28,34,37</sup>

### 3.5 | NET

NET monitoring over 72 h after the first administration of both OHP and PTX enabled it to demonstrate a different pattern,

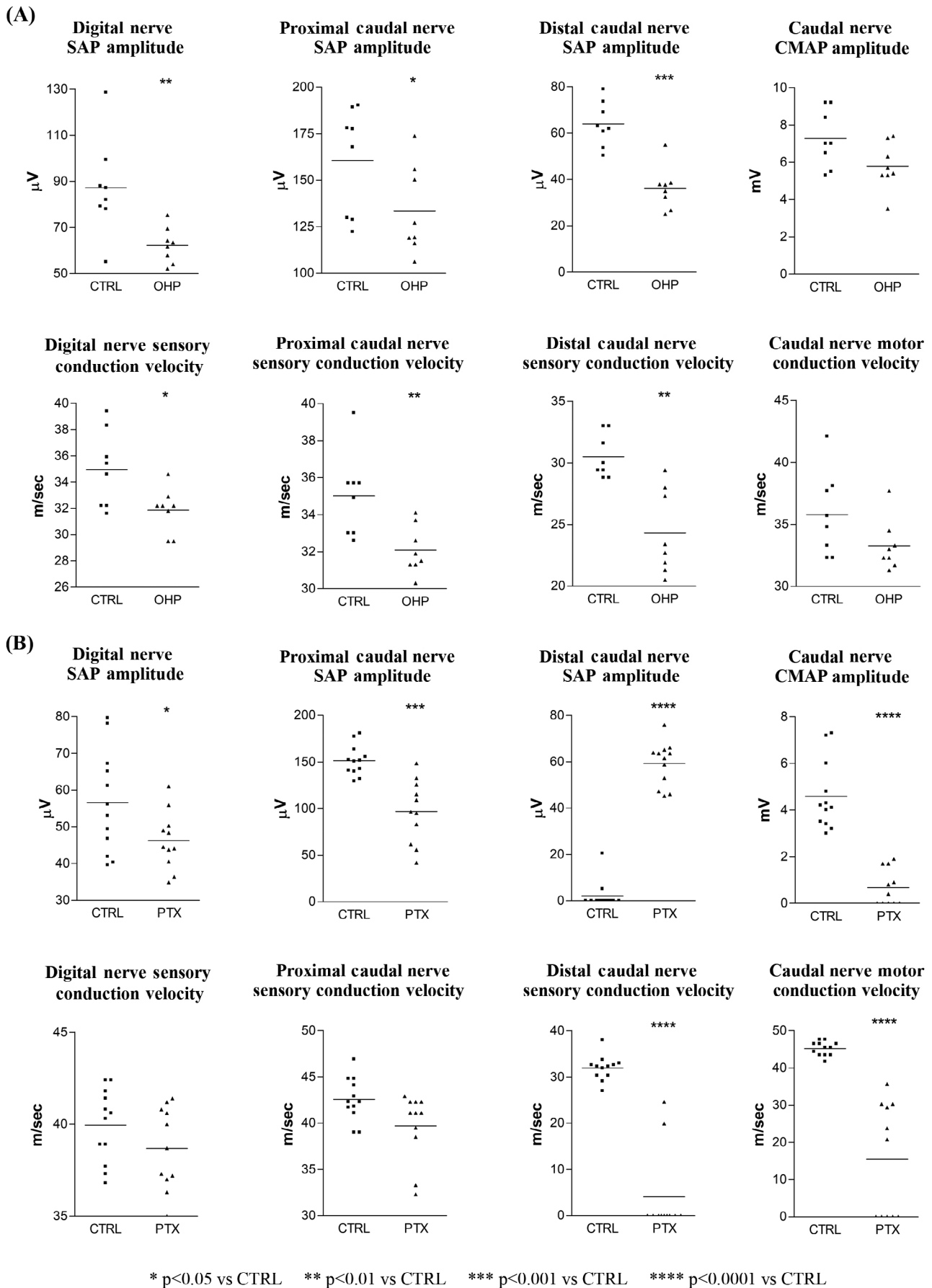
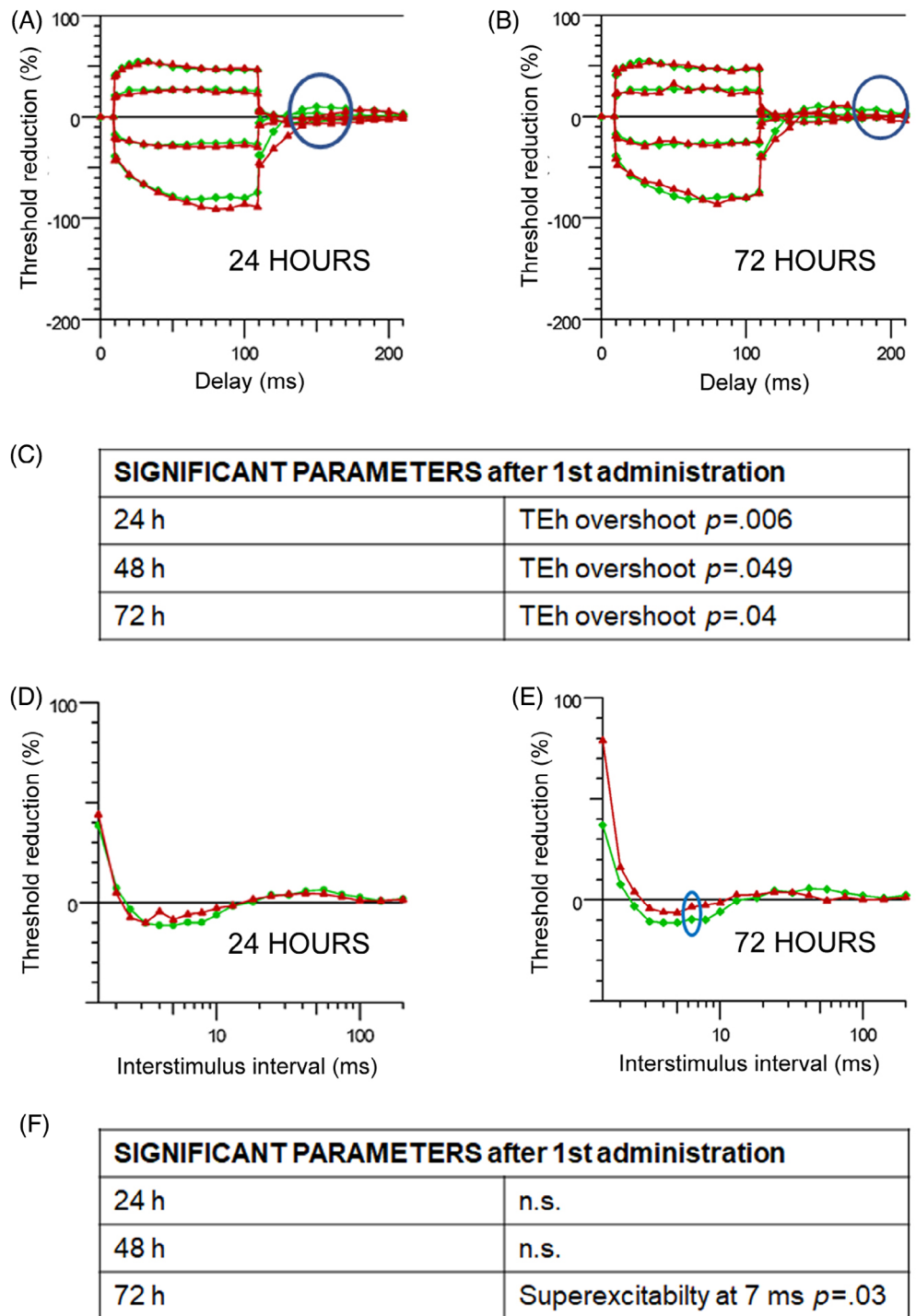


FIGURE 4 Legend on next page.

**FIGURE 5** Nerve excitability testing in OHP experiment after the first administration (CMAP of caudal nerve). Figure 5A: threshold electrotonus curves at 24 h after the first administration (green: control group; red: OHP group); Figure 5B: threshold electrotonus curves at 72 h after the first administration (green: control group; red: OHP group); Figure 5C: threshold electrotonus significant parameters over the 72 h of monitoring; Figure 5D: recovery cycle curves at 24 h after the first administration (green: control group; red: OHP); Figure 5E: recovery cycle curves at 72 h after the first administration (green: control group; red: OHP); Figure 5F: recovery cycle significant parameters over the 72 h of monitoring. CMAP: compound muscle potential; TEh: hyperpolarising threshold electrotonus. Blue circles are guiding the reader in determining the significant parameters over the curves.

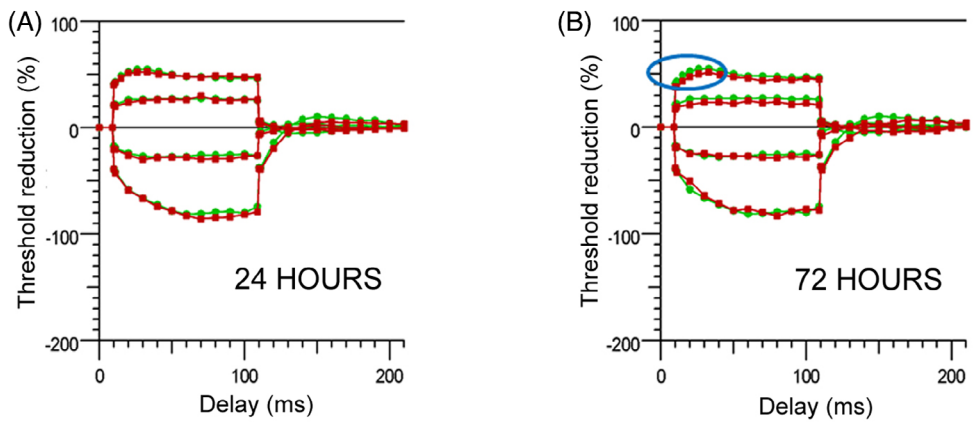


underlying the different pattern of axonopathy that would later ensue.

In the OHP experiment, as summarised in Figure 5 (see supplementary Figure 1 for data showing mean and standard deviation), we observed changes in both threshold electrotonus (TE) and

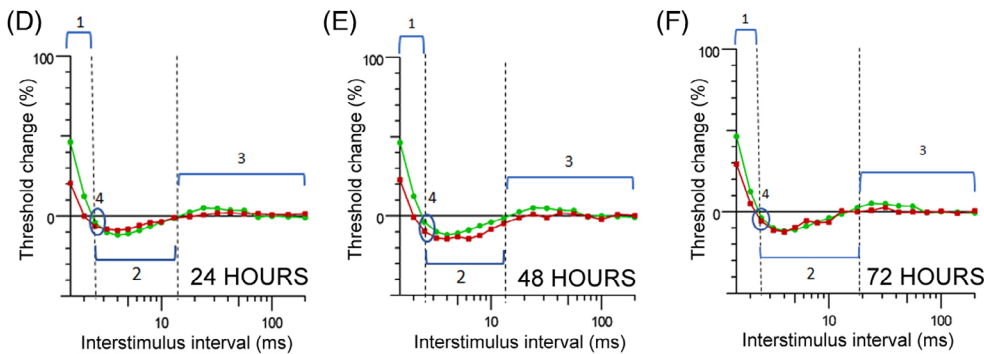
recovery cycle. For what regards TE, a relevant change in hyperpolarising TE was observed. The most notable change was, though, in the recovery cycle curve: the OHP group pattern showed the typical alterations in superexcitability (e.g., the entire curve is pulled upward), matching the known pattern of transient alterations in

**FIGURE 4** Nerve conduction study results and statistical analysis are shown. Figure 4A: OHP experiment. A mild sensory axonopathy is shown. Figure 4B: PTX experiment. A moderate-severe sensory-motor axonal polyneuropathy is shown. CMAP, compound muscle action potential; CTRL, control group; OHP, oxaliplatin group; PTX, paclitaxel group; SAP, sensory action potential.



(C)

SIGNIFICANT PARAMETERS after 1st administration	
24 h	n.s.
48 h	n.s.
72 h	TEd(10-20 ms) $p=.04$ TEd20(10-20 ms) $p=.04$



LEGEND

1. Relative refractory period (msec)
2. Superexcitability period (msec)
3. Subexcitability period (msec)
4. Refractoriness at 2.5 msec (%)

(G)

SIGNIFICANT PARAMETERS after 1st administration	
24 h	Superexcitability (%) $p=.001$ Refractoriness $p=.006$
48 h	Subexcitability (%) $p=.004$ Relative refractory period $p=.004$ Refractoriness at 2.5 $p=.004$ Refractoriness $p=.004$
72 h	Superexcitability (%) $p=.02$

sodium-voltage operated ion channels kinetics that OHP is able to induce. [5,12,18,23,30](#)

In the PTX experiment, as summarised in Figure 6 (see Supplementary Figure 2 for data showing mean and standard deviation), we observed very minor changes in TE only at 72 h, compatible with a

**FIGURE 6** Nerve excitability testing in PTX experiment after the first administration (CMAP of caudal nerve). Figure 6A: threshold electrotonus curves at 24 h after the first administration (green: control group; red: PTX group); Figure 6B: threshold electrotonus curves at 72 h after the first administration (green: control group; red: PTX group); Figure 6C: threshold electrotonus significant parameters over the 72 h of monitoring; Figure 5D: recovery cycle curves at 24 h after the first administration (green: control group; red: PTX group); Figure 6E: recovery cycle curves at 48 h after the first administration (green: control group; red: PTX group); Figure 6F: recovery cycle curves at 72 h after the first administration (green: control group; red: PTX group); Figure 6G: recovery cycle significant parameters over the 72 h of monitoring. CMAP: compound muscle potential; TEd: depolarising thresholds electrotonus. Blue circles are guiding the reader in determining the significant parameters over the curves.

reduced threshold, demonstrating a less efficient accommodation to polarisation (i.e., a trend to a 'fanned in' appearance). More prominent changes were instead observed in the recovery cycle with reduction of both super- and subexcitability, as well as in refractoriness, determining a flattening of the curves in PTX group.



## 4 | DISCUSSION

In our study we exploited NET to detect precocious axonal dysfunction due to different mechanisms leading to axonal damage, verifying changes after exposure to two different neurotoxic drugs: OHP and PTX. We exploited the known dose and time-dependent peripheral neurotoxicity of these drugs to test if NET might be suitable to early grasp meaningful functional changes before actual axonal damage is there.

OHP is known to alter ion channels/transporters balance leading to axonal damage after prolonged administration, due to a transient state of axonal hyperexcitability after each and every administration, which can be referred as an *acute* OHP-related CIPN.<sup>2,5,12</sup> Thus, NET (CMAP, caudal nerve) is an ideal choice to detect *in vivo* alterations in ion channels/transporters functioning and properties. Our data were in line with previous observations in this regard and this hyperexcitability state, despite transient, was associated with the development of the expected mild axonal damage at the end of the treatment.<sup>5</sup> CIPN onset was verified with a multimodal and refined approach combining NCS, histopathology and behavioural tests; therefore, the fact that CIPN had ensued and its severity was confirmed with a *state-of-the-art* approach.<sup>15,33</sup> This is, of course, the most immediate and obvious application NET might be thought to have in CIPN field. However, the possibility to test axonal properties as soon as the first cycle could be relevant also in settings in which a channelopathy is not present; in fact, in our PTX model, we did not observe a pattern compatible with a state of transient axonal hyperexcitability but rather with an early state of axonal dysfunction, which was then confirmed as leading to a more severe axonopathy, compared to OHP experiment, as demonstrated by NCS and histopathological analyses. NET changes observed in PTX experiment showed a *fanning in* at the threshold electrotonus and altered parameters of recovery cycle: superexcitability, subexcitability and refractoriness. The fanning in observed in our animals mirrored changes due to early diabetic neuropathy,<sup>35,36</sup> which is compatible with a reduction of the Na<sup>+</sup>/K<sup>+</sup> pump activity.<sup>36</sup> Superexcitability can be used as an indicator of the membrane potential since it mirrors the depolarisation afterpotential, whereas subexcitability reflects the hyperpolarisation of the membrane potential, reflecting slow K<sup>+</sup> currents at the node. PTX group showed a flattening of the recovery cycle, once again reflecting reduction of Na<sup>+</sup>/K<sup>+</sup> pump activity that progressively ensues in patients affected by diabetes.<sup>36</sup> It should be noted that our findings are different from the ones observed in small clinical cohorts of PTX-treated patients, but, actually, the comparison is not appropriate since in these clinical studies the authors did not test NET as soon as after the first weekly PTX cycle, but later on during chemotherapy<sup>29</sup> or even after.<sup>25</sup>

One of the main novelties of our study is that we recorded NET soon after the first cycle allowing us the best chance to detect changes predictive of axonal damage at the end of the treatment far before the actual axonal damage is ongoing. Therefore, our observations have potentially a highly translational profile, since NET can be similarly performed in clinical trials. One of the major issues in designing a preventive clinical trial in CIPN is enrolling patients who will actually develop peripheral neuropathy, since not all patients

will experience CIPN and, even if neurotoxicity ensues, its severity can vary.<sup>4,7,10,28</sup> We already proposed the longitudinal monitoring of the dorsal sural nerve at mid-treatment to detect patients at higher risk to develop neuropathy in a clinical setting,<sup>6</sup> but it would be far more valuable to have a tool that even more precociously can detect changes predictive of axonal damage, as NET was demonstrated to be doing in our preclinical *proof-of-concept* study. Furthermore, differently from serum biomarkers such as neurofilament light chain (NFL) levels,<sup>8</sup> that can only detect axonal damage onset, NET provides dynamic observations of axonal properties allowing to perform both *in vivo* experiments and in clinical research setting observations mirroring the different pathogenetic mechanisms that are undergoing; in fact, as demonstrated by our data, NET elegantly detected both the OHP-related channelopathy and the precocious functional axonal dysfunction due to PTX, matching the different ongoing axonal damage. Thus, it could be suggested that NET should be further explored as a precious link between bench and bedside for research purposes: in fact, at bench side, all hypotheses just indirectly inferred via NET on axonal damage can be directly confirmed via histopathology and biomolecular techniques. Thus, applying NET as soon as the first cycle might be of interest in specifically designed neuroprotection clinical trials: it could enable to detect patients with an actual ongoing and precocious axonal dysfunction before actual axonal damage ensues; this will avoid to include patients who will not develop any sign/symptoms of neuropathy at the end of the treatment. In principle, this could be applied to other settings than CIPN, as an example, in patients affected by other neuropathies that slowly develops over time (e.g., related to diabetes) to best select patients to be enrolled in a preventive (not curative) clinical trial: NET could inform on such precocious changes before axonal damage actually occurs, but still pointing out patients who will actually develop some and, therefore, are the appropriate population to be screened for enrolment.

### ACKNOWLEDGMENTS

Paola Alberti is supported by Fondazione Cariplo's grant Biomedical Research conducted by Young Researchers.

### CONFLICT OF INTEREST STATEMENT

Authors have nothing to disclose.

### DATA AVAILABILITY STATEMENT

The data that support the findings of this study are available from the corresponding author upon reasonable request.

### ORCID

Cristina Meregalli  <https://orcid.org/0000-0002-4281-4577>

Guido Cavaletti  <https://orcid.org/0000-0003-4128-2406>

Paola Alberti  <https://orcid.org/0000-0001-6106-6183>

### REFERENCES

1. Alberti P. Chemotherapy-induced peripheral neurotoxicity-outcome measures: the issue. *Expert Opin Drug Metab Toxicol*. 2017;13:241-243.

2. Alberti P. Platinum-drugs induced peripheral neurotoxicity: clinical course and preclinical evidence. *Expert Opin Drug Metab Toxicol.* 2019;15:487-497.
3. Alberti P. Role of neurophysiology in chemotherapy-induced peripheral neuropathy (CIPN). *Clin Neurophysiol.* 2020;131:1964-1965.
4. Alberti P, Bernasconi DP, Cornblath DR, Merkies ISJ, Park SB, Velasco R, Bruna J, Psimaras D, Koeppen S, Pace A, Dorsey SG, Argyriou AA, Kalofonos HP, Briani C, Schenone A, Faber CG, Mazzeo A, Grisold W, Valsecchi M, Cavaletti G, group C-P (2021) Prospective evaluation of health care provider and patient assessments in chemotherapy-induced peripheral neurotoxicity. *Neurology* 97:e660-e672.
5. Alberti P, Canta A, Chiorazzi A, et al. Topiramate prevents oxaliplatin-related axonal hyperexcitability and oxaliplatin induced peripheral neurotoxicity. *Neuropharmacology.* 2020;164:107905.
6. Alberti P, Rossi E, Argyriou AA, et al. Risk stratification of oxaliplatin induced peripheral neurotoxicity applying electrophysiological testing of dorsal sural nerve. *Support Care Cancer.* 2018;26:3143-3151.
7. Alberti P, Salvalaggio A, Argyriou AA, et al. Neurological complications of conventional and novel anticancer treatments. *Cancers (Basel).* 2022;14:60888.
8. Alberti P, Semperboni S, Cavaletti G, Scuteri A. Neurons: the interplay between cytoskeleton, ion channels/transporters and mitochondria. *Cells.* 2022;11:2499.
9. Argyriou AA, Park SB, Islam B, Tamburin S, Velasco R, Alberti P, Bruna J, Psimaras D, Cavaletti G, Cornblath DR, (TNC) TNC (2019) Neurophysiological, nerve imaging and other techniques to assess chemotherapy-induced peripheral neurotoxicity in the clinical and research settings. *J Neurol Neurosurg Psychiatry.* 2019;90:1361-1369.
10. Argyriou AA, Velasco R, Briani C, et al. Peripheral neurotoxicity of oxaliplatin in combination with 5-fluorouracil (FOLFOX) or capecitabine (XELOX): a prospective evaluation of 150 colorectal cancer patients. *Ann Oncol.* 2012;23:3116-3122.
11. Arnold R, Moldovan M, Rosberg MR, Krishnan AV, Morris R, Krarup C. Nerve excitability in the rat forelimb: a technique to improve translational utility. *J Neurosci Methods.* 2017;275:19-24.
12. Ballarini E, Malacrida A, Rodriguez-Menendez V, et al. Sodium-calcium exchanger 2: a pivotal role in oxaliplatin induced peripheral neurotoxicity and axonal damage? *Int J Mol Sci.* 2022;23:10063.
13. Bostock H, Cikurel K, Burke D. Threshold tracking techniques in the study of human peripheral nerve. *Muscle Nerve.* 1998;21:137-158.
14. Boërio D, Greensmith L, Bostock H. Excitability properties of motor axons in the maturing mouse. *J Peripher Nerv Syst.* 2009;14:45-53.
15. Bruna J, Alberti P, Calls-Cobos A, Caillaud M, Damaj MI, Navarro X. Methods for in vivo studies in rodents of chemotherapy induced peripheral neuropathy. *Exp Neurol.* 2020;325:113154.
16. Burke D, Mogyoros I, Vagg R, Kiernan MC. Quantitative description of the voltage dependence of axonal excitability in human cutaneous afferents. *Brain.* 1998;121(Pt 10):1975-1983.
17. Griffith KA, Dorsey SG, Renn CL, et al. Correspondence between neurophysiological and clinical measurements of chemotherapy-induced peripheral neuropathy: secondary analysis of data from the CI-PeriNomS study. *J Peripher Nerv Syst.* 2014;19:127-135.
18. Heide R, Bostock H, Ventzel L, et al. Axonal excitability changes and acute symptoms of oxaliplatin treatment: in vivo evidence for slowed sodium channel inactivation. *Clin Neurophysiol.* 2018;129:694-706.
19. Hershman DL, Lacchetti C, Dworkin RH, Lavoie Smith EM, Bleeker J, Cavaletti G, Chauhan C, Gavin P, Lavino A, Lustberg MB, Paice J, Schneider B, Smith ML, Smith T, Terstriep S, Wagner-Johnston N, Bak K, Loprinzi CL, Oncology ASoc (2014) Prevention and management of chemotherapy-induced peripheral neuropathy in survivors of adult cancers: American Society of Clinical Oncology clinical practice guideline. *J Clin Oncol* 32:1941-1967.
20. Hill A, Bergin P, Hanning F, et al. Detecting acute neurotoxicity during platinum chemotherapy by neurophysiological assessment of motor nerve hyperexcitability. *BMC Cancer.* 2010;10:451.
21. Krishnan AV, Goldstein D, Friedlander M, Kiernan MC. Oxaliplatin and axonal Na<sup>+</sup> channel function in vivo. *Clin Cancer Res.* 2006;12:4481-4484.
22. Loprinzi CL, Lacchetti C, Bleeker J, et al. Prevention and management of chemotherapy-induced peripheral neuropathy in survivors of adult cancers: ASCO guideline update. *J Clin Oncol.* 2020;38:3325-3348.
23. Makker PGS, White D, Lees JG, et al. Acute changes in nerve excitability following oxaliplatin treatment in mice. *J Neurophysiol.* 2020;124:232-244.
24. Maurer K, Bostock H, Koltzenburg M. A rat in vitro model for the measurement of multiple excitability properties of cutaneous axons. *Clin Neurophysiol.* 2007;118:2404-2412.
25. McCrary JM, Goldstein D, Sandler CX, et al. Exercise-based rehabilitation for cancer survivors with chemotherapy-induced peripheral neuropathy. *Support Care Cancer.* 2019;27:3849-3857.
26. Monza L, Fumagalli G, Chiorazzi A, Alberti P. Addressing the need of a translational approach in peripheral neuropathy research: morphology meets function. *Brain Sci.* 2021;11:139.
27. Monza L, Fumagalli G, Chiorazzi A, Alberti P. Translating morphology from bench side to bed side via neurophysiology: 8-min protocol for peripheral neuropathy research. *J Neurosci Methods.* 2021;363:109323.
28. Park SB, Cetinkaya-Fisgin A, Argyriou AA, Höke A, Cavaletti G, Alberti P. Axonal degeneration in chemotherapy-induced peripheral neurotoxicity: clinical and experimental evidence. *J Neurol Neurosurg Psychiatry.* 2023;94:962-972.
29. Park SB, Lin CS, Krishnan AV, Friedlander ML, Lewis CR, Kiernan MC. Early, progressive, and sustained dysfunction of sensory axons underlies paclitaxel-induced neuropathy. *Muscle Nerve.* 2011;43:367-374.
30. Park SB, Lin CS, Krishnan AV, Goldstein D, Friedlander ML, Kiernan MC. Oxaliplatin-induced neurotoxicity: changes in axonal excitability precede development of neuropathy. *Brain.* 2009;132:2712-2723.
31. Park SB, Tamburin S, Schenone A, et al. Optimal outcome measures for assessing exercise and rehabilitation approaches in chemotherapy-induced peripheral-neurotoxicity: systematic review and consensus expert opinion. *Expert Rev Neurother.* 2022;22:65-76.
32. Percie du Sert N, Hurst V, Ahluwalia A, et al. The ARRIVE guidelines 2.0: updated guidelines for reporting animal research. *BMJ Open Sci.* 2020;4:e100115.
33. Pozzi E, Fumagalli G, Chiorazzi A, et al. The relevance of multimodal assessment in experimental oxaliplatin-induced peripheral neurotoxicity. *Exp Neurol.* 2020;334:113458.
34. Pozzi E, Monza L, Ballarini E, et al. Morpho-functional characterisation of the rat ventral caudal nerve in a model of axonal peripheral neuropathy. *Int J Mol Sci.* 2023;24:1687.
35. Sung JY, Park SB, Liu YT, et al. Progressive axonal dysfunction precedes development of neuropathy in type 2 diabetes. *Diabetes.* 2012;61:1592-1598.
36. Sung JY, Tani J, Chang TS, Lin CS. Uncovering sensory axonal dysfunction in asymptomatic type 2 diabetic neuropathy. *PLoS One.* 2017;12:e0171223.
37. Tamburin S, Park SB, Alberti P, Demichelis C, Schenone A, Argyriou AA. Taxane and epothilone-induced peripheral neurotoxicity: from pathogenesis to treatment. *J Peripher Nerv Syst.* 2019;24-(Suppl 2):S40-S51.
38. Tamburin S, Park SB, Schenone A, et al. Rehabilitation, exercise, and related non-pharmacological interventions for chemotherapy-induced peripheral neurotoxicity: systematic review and evidence-based recommendations. *Crit Rev Oncol Hematol.* 2022;171:103575.
39. Velasco R, Bruna J. Taxane-induced peripheral neurotoxicity. *Toxics.* 2015;3:152-169.

40. Wild BM, Morris R, Moldovan M, Krarup C, Krishnan AV, Arnold R. In vivo electrophysiological measurement of the rat ulnar nerve with axonal excitability testing. *J Vis Exp*. 2018;132:56102.
41. Yang Q, Kaji R, Hirota N, et al. Effect of maturation on nerve excitability in an experimental model of threshold electrotonus. *Muscle Nerve*. 2000;23:498-506.

#### SUPPORTING INFORMATION

Additional supporting information can be found online in the Supporting Information section at the end of this article.

**How to cite this article:** Chiorazzi A, Canta A, Carozzi VA, et al. Morphofunctional characterisation of axonal damage in different rat models of chemotherapy-induced peripheral neurotoxicity: The role of nerve excitability testing. *J Peripher Nerv Syst*. 2024;29(1):47-57. doi:[10.1111/jns.12607](https://doi.org/10.1111/jns.12607)